Hindawi
Advances in Materials Science and Engineering
Volume 2019, Article ID 3829281, 19 pages
https://doi.org/10.1155/2019/3829281

Review Article

A Comprehensive Review of the Mechanical Behavior of Suspension Bridge Tunnel-Type Anchorage

Yafeng Han,[1,2] Xinrong Liu,[1,2] Ning Wei,[1,2] Dongliang Li,[3] Zhiyun Deng,[1,2] Xiangchao Wu,[1,2] and Dongshuang Liu[1,2]

[1]*School of Civil Engineering, Chongqing University, Chongqing 400045, China*
[2]*National Joint Engineering Research Center of Geohazards Prevention in the Reservoir Areas (Chongqing), Chongqing 400045, China*
[3]*Commission of Housing and Urban-rural Development of Banan District, Chongqing 400055, China*

Correspondence should be addressed to Xinrong Liu; liuxrong@126.com

Received 27 February 2019; Revised 11 July 2019; Accepted 6 September 2019; Published 9 October 2019

Academic Editor: José António Fonseca de Oliveira Correia

The recent surge of interest towards the mechanical response of rock mass produced by tunnel-type anchorage (TTA) has generated a handful of theories and an array of empirical explorations on the topic. However, none of these have attempted to arrange the existing achievements in a systematic way. The present work puts forward an integrative framework laid out over three levels of explanation and practical approach, mechanical behavior, and calculation method of the ultimate pullout force to compare and integrate the existing findings in a meaningful way. First, it reviews the application of TTA in China and analyzes its future development trend. Then, it summarizes the research results of TTA in terms of load transfer characteristics, deformation characteristics, failure modes, and calculation of ultimate uplift resistance. Finally, it introduces four field model tests in soft rock (mainly mudstone formations), and some research results are obtained. Furthermore, it compares the mechanical behavior of TTA in hard rock strata and soft rock strata, highlighting the main factors affecting the stability of TTA in soft rock formation. This paper proposes a series of focused topics for future investigation that would allow deconstruction of the drivers and constraints of the development of TTA.

1. Introduction

China proposed "The Great Western Development (GWD)" strategy and "The Belt and Road" initiative in 1999 and 2013, respectively [1, 2], with the aim to promote the gradual shift of China's infrastructure construction to western mountainous terrains with complex geological conditions. The topographic unit of China's southwest region (i.e. Chongqing City, Guizhou Province, Yunnan Province, Sichuan Province, and Tibet Autonomous Region) is mountains. This region features high mountains and steep slopes, vertical and horizontal valleys, and complex river networks, which makes the bridges crucial for crossing valleys and rivers and for allowing land communication.

Cable-supported bridges come in cable-stayed and suspension forms; one of the main forms of long-span bridges are suspension bridges [3, 4], which are one of the main models [5], because it has significant advantages in exerting material properties and height-span ratio of stiffening girder. Being flexible, suspension bridges are mainly composed of main beam, tower pier, cable, and anchorage, in which anchorage is the key structure of anchoring main cable of suspension bridge [6] (Figure 1). Suspension bridge can be classified as self-anchored suspension and ground-anchored suspension [7]. The first, the self-anchored suspension bridge anchors the main cable at the end of the stiffening girder, and the stiffening girder bears the horizontal and vertical forces; the second is a system that transfers the main cable tension to the rock mass or directly

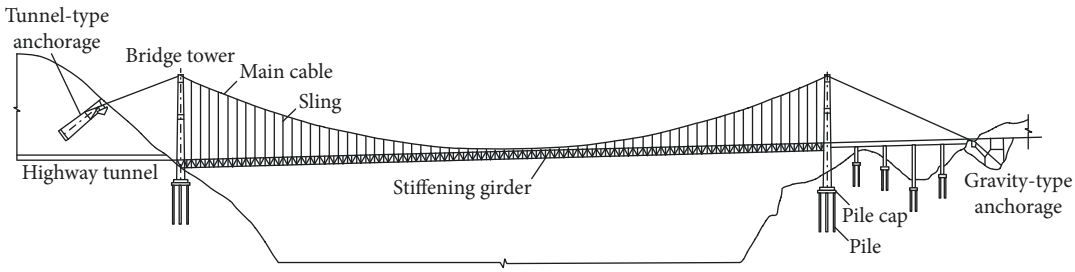

Figure 1: Structural diagram of suspension bridge.

balances the main cable tension through the anchorage's weight. The anchorage of ground anchorage suspension bridge can be divided into two types: gravity-type anchorage (GTA) and tunnel-type anchorage (TTA) according to the difference of anchorage structure and loading character.

GTAs mainly rely on the gravity of mass concrete anchorages and the friction between anchorages and the horizontal plane of the foundation to counteract the tension of the main cable. The bearing mechanism is simple, but the huge amount of earth and rock excavation and concrete consumption bring high construction cost and huge environmental burden. A TTA is a concrete plug body with a wedge shape that is large at the bottom and small at the top. The main cable force can be transferred to the rock mass through the plug body. TTAs have a very different application technology and loading mechanism from that of GTAs, and can have the same bearing capacity as GTAs at a smaller project scale (the volume of TTAs is only 20% or 25% of GTAs); so, TTA works as an anchorage with high performance-price ratio and little disturbance to the surrounding environment [8]. The tunnel-type anchorage may be preferable in view of space and environmental concerns [9]. The recommendatory standard of "Specifications for Design of Highway Suspension Bridges" [10] suggests that when the geological conditions of the anchorage site are good and when the terrain is conducive to the layout of a TTA, the feasibility of constructing TTAs should first be considered.

At present, research on large-span suspension bridges focus on bridge design techniques [11, 12], structural response under wind or dynamic loading [13–16], bridge structure health monitoring and risk assessment [17–20], and bridge foundation deformation and stability [21, 22]. The TTA is an environment-friendly and cost-effective anchorage form, but due to its relatively high requirements on geological conditions, its application in suspension bridges remains relatively limited.

Because of the special geometry of the plug body, there is a complex interaction between the surrounding rock and the plug body. The complexity increases also due to constraints of the test conditions, test means, numerical simulation technology, and the level of theoretical development, etc. For this reason, the TTAs still have some shortcomings in some key problems such as load transfer character, deformation evolution law, failure mode, and the calculation method of ultimate pullout force, which to some extent limit the application of TTA. Many scholars have carried out some theoretical and empirical researches on such deficiencies and have obtained a lot of research results. However, there is a lack of systematic summary and analysis of the existing achievements, and a lack of systematic thinking on the future research topics of TTA.

Based on the statistical analysis of a large number of bridge cases and the application of TTAs in China, this paper summarizes and analyzes the research results of TTAs in bearing deformation characteristics, failure modes, and calculation methods of ultimate uplift resistance. At the same time, based on some research achievements of the author in recent years, this paper also analyzes the bearing deformation characteristics, long-term stability, and failure mode of TTAs in soft rock strata, comparing the difference of mechanical behavior of TTA in soft rock formation and hard rock formation. Finally, a series of topics about future researches in TTA is introduced.

2. Anchorage Types

The gravity of anchorage and the friction between the anchorage and foundation are the sources of the pullout force of GTA. Figure 2(a) shows the schematic of GTA. For GTAs, some advantages such as simple construction, reliable operation, simple bearing mechanism, and vast application are easily found. Nevertheless, some disadvantages such as huge excavation volume, high cost, and serious damage to ecological environment also should not be neglected. For rock anchorage (see Figure 2(b)), the dispersed cable is anchored in rock mass. The concrete anchorage is not used in the anchor frame. The excavation volume of rock anchorage construction is less and the damage to ecological environment is slight. However, stress concentration is easily appeared in the rock mass due to the smaller stress range. Additionally, the construction technology of rock anchorage is also complex. This anchorage is usually suitable for the hard rock strata with simple structures, good geological conditions, or intact rock mass. The structure of the compound anchorage is shown in Figure 2(c). The dispersed cable is anchored in concrete plug body and rock mass. The wedge-shaped plug body can fully drive the rock mass to bear the load and change the surrounding rock mass into a part of the bearing structure.

TTA is mainly composed of cable, splay saddle, plug body, front room, and rear room (Figures 2(d) and 2(e)). The cable is the main carrier to transfer the load of the bridge and the main load-bearing component of the suspension bridge,

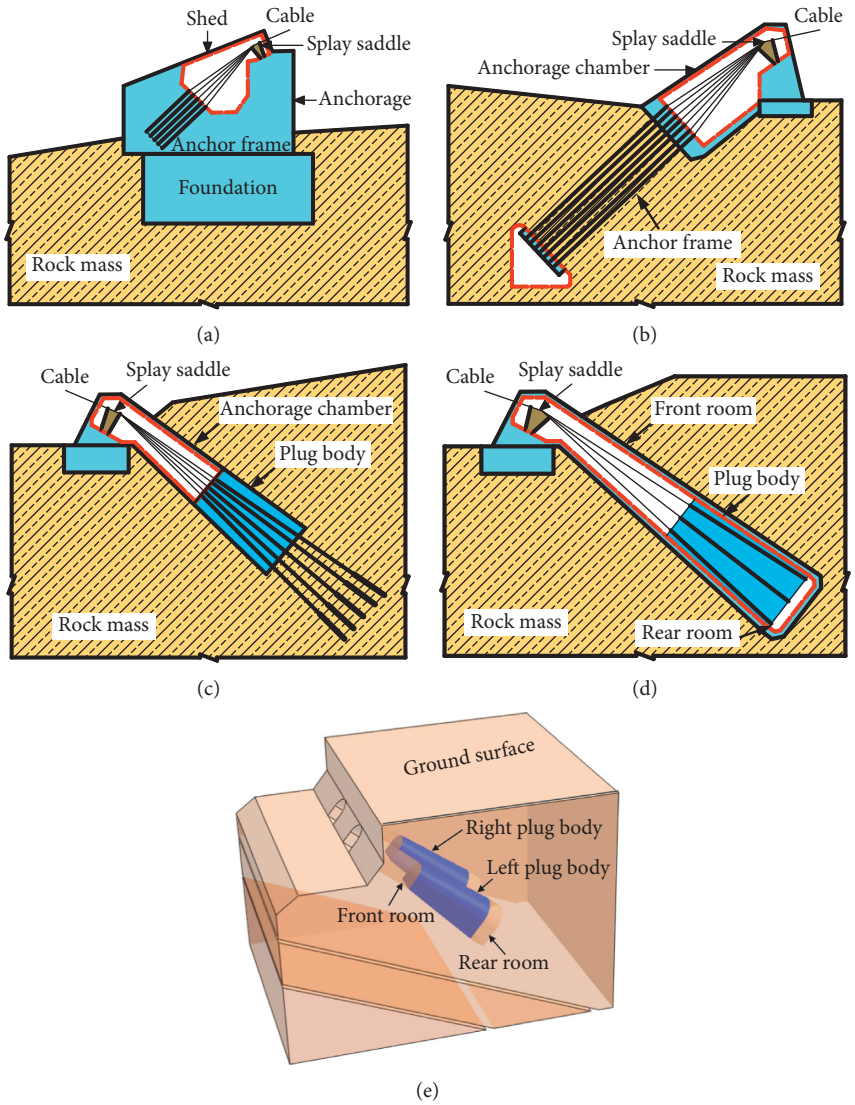

Figure 2: (a) Gravity-type anchorage. (b) Rock anchorage. (c) Compound anchorage. (d) Tunnel-type anchorage. (e) Schematic of spatial arrangement of TTA.

which is generally made of galvanized high-strength steel wire. The splay saddle is a concrete component that supports the main cable and changes the direction of the cable smoothly. After passing the splay saddle, the cable is dispersed into an ensemble of single strands, which are inserted into the plug body at a certain angle. The plug body is the key component to transfer the cable force to the surrounding that bears the loads.

3. Application Situation

TTA was firstly applied in the Washington Bridge built in 1932 [23, 24]. Four years later, the United States built a second suspension bridge with TTAs in the San Francisco Bay area, i.e. the Oakland-San Francisco Bay Bridge [25, 26]. In 1964, Britain built the Forth Road Bridge across Foss Bay [27], becoming the second country after the United States to use TTAs in suspension bridges. Japan built the Shimotsui-Seto Bridge between Honshu and Shikoku in 1988 across the Seto Inland Sea [28]. In addition, there are Norway's Cavalsson Bridge, the Riviera Viaduct in Central Sweden, and the South Korean Bridge in Ulsan Port, in all of which TTA is used in engineering practice.

Although the construction of modern suspension bridge with TTA in China started later, the mechanism has been developed for more than 20 years and the country has made brilliant achievements in this field. This paper summarizes the anchoring form of 113 suspension bridges with span over 90 m in China (Figure 3(a)), of which 33 are self-anchored suspension bridges, accounting for 29.22% of the total number of bridges. There are 80 ground-anchored suspension bridges, accounting for 70.8% of the total number of bridges. Most of the loads of ground-anchored suspension bridges are borne by anchorage or surrounding rock mass; so, the main girder of the bridge body is less stressed, which avoids large deformation or instability of the main girder

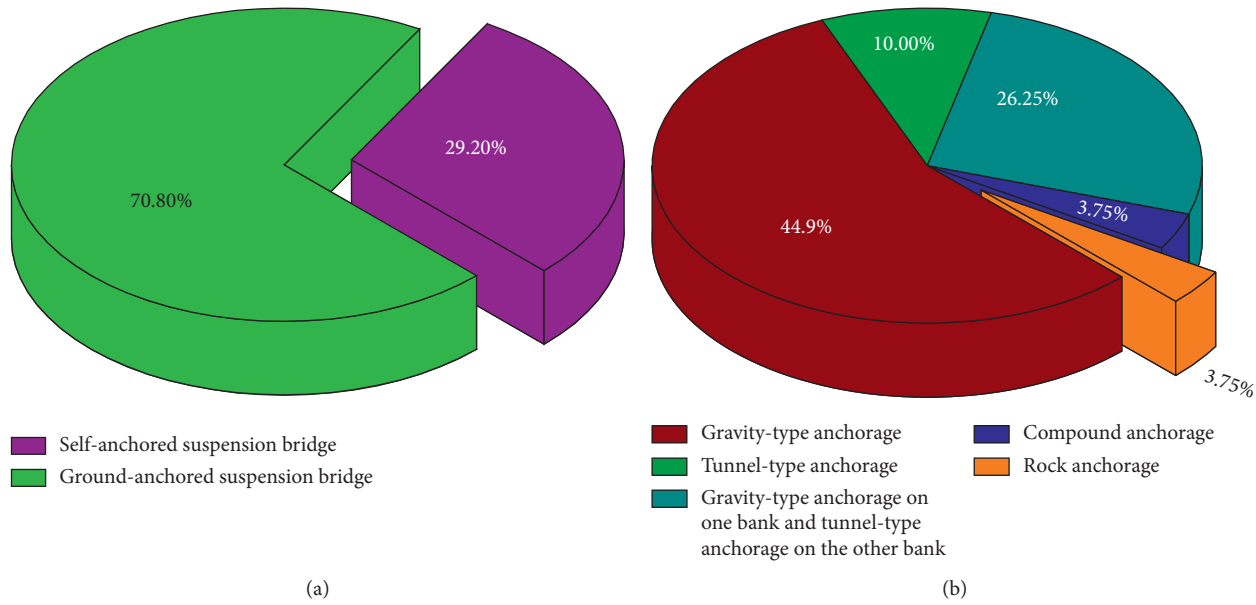

Figure 3: (a) Proportion of self-anchored and ground-anchored suspension bridge. (b) Statistical results of anchorage form of ground-anchored suspension bridge.

caused by the large load of the long-span bridge, increasing the strength of the spanning capability [29]. At present, the bridge with the largest span in the world is Japan's Akashi-Kaikyo Bridge (1991 m), which adopts ground-anchored suspension bridge system. Among the 80 ground-anchored suspension bridges in statistics (Figure 3(b)), there are 45 suspension bridges with GTAs on both banks of the bridge, accounting for 44.9% of the total number of bridges. There are 8 suspension bridges with TTA, accounting for 10% of the total number of bridges. There are 21 suspension bridges with TTA on the other bank, accounting for 26.25% of the total number of bridges. The suspension bridges with pre-stressed composite anchorage and rock anchorage are adopted on both banks of the bridge, each accounting for 3.75% of the total number of bridges.

Based on the year of completion for some ground-anchored suspension bridges (76 in total) built in China from 1981 to 2020, the percentage of suspension bridges built with TTAs (including suspension bridges built with TTAs on both banks or only one bank) in the bridges completed in every five years is calculated, and the statistical results are shown in Figure 4.

Among the suspension bridges with TTAs, some bridges use TTAs on both banks of the bridge, while some bridges use TTAs on one bank and GTAs on the other. The proportion of the two types of suspension bridges is shown in Figure 4(a). According to Figure 4(a), the suspension bridge constructed by "TTA + GTA" accounts for the highest proportion, followed by the suspension bridge with TTA on both banks. It can be seen from Figure 4(b) that the proportion of suspension bridges built with TTAs in each stage is increasing, and TTAs are being increasingly applied to suspension bridges.

Table 1 shows the statistical results of 29 TTAs in China. By comparison, it is found that TTAs are applied in a wider area that is not limited to hard rock formations and simple geological structure; instead, there is a tendency to extend in soft rock stratum or poor quality rock mass.

4. Mechanical Behavior of TTA

The mechanical behavior of tunnel-type anchorages is similar for that of the piles (or rock anchors), especially with enlarged bottoms piles. Many model tests and numerical simulations were conducted to investigate the design methods, deformation characteristics, failure modes, and failure mechanics of uplift piles [30–32]. However, the topological shape of a wedge-shaped plug body differs from that of uplift piles with a constant section or belled uplift piles. When bearing loads, uplift piles are in a vertical state, whereas the plug bodies of a tunnel-type anchorage are inclined.

There are complicated interactions between the plug body and surrounding rock due to the special wedge-shaped structure of plug body. The plug body is the medium transferring the main cable force to the surrounding rock. The load transfer characteristics and deformation characteristics of TTA were usually paid more attention, which helped us to understand the mechanical behavior of TTA better.

4.1. Load Transfer Characteristics of TTA. At present, what we already know about the TTA load transfer is, first, the clamping effect [33], and the second, the wedge effect [34]. The two effects share the same connotations. TTA is a component that transfers the tension of the main cable to the surrounding rock through a concrete plug body with a wedge shape that is large at the bottom and small at the top. The plug body can fully drive the surrounding rock mass to

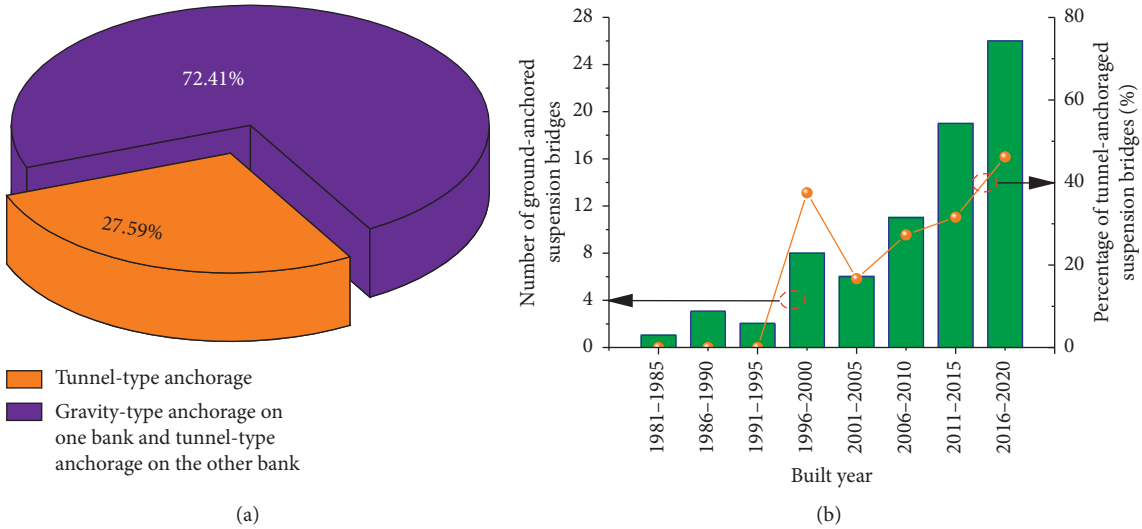

(a) (b)

Figure 4: (a) The proportion of suspension bridge with TTA on both banks and only one bank. (b) Development trend of TTA.

bear load and change the surrounding rock mass into a part of the bearing structure to form a composite bearing system of "plug body + surrounding rock." The surrounding rock around the plug body is in the state of compression-shear stress. Under this stress state, the surrounding rock can hold the plug body to resist the large drawing force because of the shear expansion and strain hardening property of the rock mass.

Clamping effect coefficient is defined to quantitatively describe the degree of the clamping effect [35]. It is the ratio of the ultimate pullout resistance of the TTA using the wedge-shaped plug body and cylinder plug body. Li [36] obtained the theoretical calculation formula of clamping effect coefficient through theoretical derivation.

4.2. Deformation Characteristics of TTA. As shown in Figure 5(a) [33, 37], on the back end of the plug body, the surface displacement of the back face of the two plug bodies (S_3 and S_5) is larger than the surface displacement of the rock mass between the plug bodies (S_4) and on both sides of the plug bodies (S_1, S_2, S_6 and S_7) in the pull direction. The surface displacement of the rock mass between the plug bodies is also greater than that on both sides of the plug bodies. The surface displacement distribution curve of the rock mass in the pull direction approximately presents a symmetrical bimodal at the center of the rock mass between the plug bodies. On the front end of the plug body, the surface displacement distribution curve of the rock mass in the pull direction approximately presents a single peak [33] or a symmetrical bimodal [8, 38–40] at the center of the rock mass between the plug bodies. The shape of the displacement distribution curve depends on the attenuation degree of the load passing through the plug body.

For the deformation of the plug body [41] (Figure 5(b)), the maximum axial displacement of the back face or front face is located at the arch top, and the axial displacement of the back face is greater than that of the front face. In addition, the displacement of plug body in the pull direction is the largest, followed by the vertical displacement. The smallest displacement is in the lateral one [41].

Field model test is one of the main methods to study the deformation characteristics of TTA. However, the effect of large-scale model test is often not satisfactory as it is influenced by many factors and its experimental conditions are difficult to control. For example, in field model tests of TTAs of the Puli Bridge (the geometric similarity ratio of the prototype and the model is CL = 25), the surrounding rock was still in the elastic state when the pushing jack was working at full load [33]. The rope was broken during the field model test (CL = 12.5) of TTA of the E'gongyan Bridge in Chongqing, and the test was forced to be terminated [42]. In field model tests of TTAs of the Sidu River Bridge (CL = 12), the maximum load during test was only 6P [43] (2P represents twice the design load), and the average additional stress and deformation of rock mass measured were very small. Limited by the test equipment and the geological conditions of the anchorage site, most of the above model tests were terminated when they were only loaded to the elastic stage of surrounding rock. The deformation characteristics and failure mode of TTA under plastic and even ultimate failure conditions cannot be clearly understood. In addition, the "size effect" of field model test will also have a significant impact on the test results [44].

With the help of numerical calculation software, it is easy to obtain the load-bearing deformation characteristics of the TTA in the whole process of elasticity-plasticity failure. The discrete element simulation method has some advantages in the analysis of nonlinear and large deformation problems in discontinuous media. Studies on the deformation and failure of TTA using discrete element software can be carried out together with model test for mutual verification, which is helpful to further reveal the key problems such as load transfer mechanism, deformation evolution law, and failure mechanism of TTA. However, the current research in this area is rare.

Table 1: Information on suspension bridges built by TTAs in China.

Name of bridge (completed year)	Rock stratum condition in anchorage site
Fengdu Yangtze River Bridge (1997)	TTA is adopted on both banks of the bridge. The length of the plug body is 10 m, and the rock mass of the north bank anchorage site is composed of moderately to slightly weathered feldspar quartz sandstone with undeveloped cracks. The surrounding rock of the anchorage site on the south bank is mainly composed of muddy sandstone
E'gongyan Bridge (2000)	TTA is adopted on the east bank of the bridge. The length of the plug body is 42 m, and the anchorage site is interbedded with soft to hard silty mudstone and quartz sandstone
Zhongxian Yangtze River Bridge (2001)	Compound anchorage is adopted on both banks of the bridge. The length of plug body is 10 m. The strata of anchorage site are mainly composed of sandstone, mudstone, and siltstone, and has simple geological structure
Wanzhou Yangtze River Bridge No. 2 (2003)	Compound anchorage is adopted on both banks of the bridge. The length of the plug body is 20 m
Jiaolongba Bridge (2005)	TTA is adopted on both banks of the bridge. The length of plug body is 13 m, and the rock mass of anchorage site is mainly composed of basalt with extremely broken rock mass, developed joints, and poor integrity
Yichang side of Sidu River Bridge (2009)	TTA is adopted on the bridge. The length of plug body is 40 m, and the rock mass in the anchorage site is hard to relatively hard limestone with less cracks and more calcium muddy filling
Balinghe Bridge (2009)	Compound anchorage is adopted on the west bank of the bridge. The length of the plug body is 40 m, and the rock mass in the anchorage site is mainly composed of slightly weathered micronew mudstone and dolomite with relatively broken surrounding rock
Nezha Bridge (2010)	TTA is adopted on both banks of the bridge. The length of the plug body is 22 m, and the rock mass in the anchorage site is composed of limestone with stable bedrock. The geological conditions of anchorage site are simple.
Aizhai Bridge (2012)	TTA is adopted on the Chadong bank of the bridge. The length of plug body is 35 m, and the rock mass of the anchorage site is composed of breezy layered limestone with developed surface corrosion crack
Nanxi Yangtze River Bridge (2008)	Compound anchorage is adopted on the bridge. The length of plug body is 25 m, and the rock mass in the anchorage site is composed of weakly to strongly weathered sandy mudstone with relatively complete rock mass
Lancang River Bridge (2013)	TTA is adopted on both banks of the bridge. The length of anchorage plug body is 15 m, and the rock mass of anchorage site is composed of weathered sandstone with broken rock mass
Wu River Bridge (2014)	TTA is adopted on the Jinsha bank of the bridge. The length of plug body is 18 m, and the rock mass of anchorage site is composed of limestone with good integrity and high strength
Prit Bridge (2015)	TTA is adopted on the Puli bank of the bridge. The length of plug body is 35 m, and the rock mass in the anchorage site is limestone
Zhangjiajie Grand Canyon Glass Bridge (2015)	TTA is adopted on the west bank of the bridge. The length of plug body is 13.5 m, and the rock mass of anchorage site is composed of breezy limestone

Table 1: Continued.

Name of bridge (completed year)	Rock stratum condition in anchorage site
Guanshan Bridge (2015)	TTA is adopted on the island bank of the bridge. The length of plug body is 27 m, and the anchorage site is composed of breezy stream porphyry with dense secondary joint. The rear room is below the sea level, and the plug body may be eroded by water
Jijiang Yangtze River Bridge (2016)	TTA is adopted on the north bank of the bridge. The length of plug body is 60 m, and the rock mass of anchorage site is composed of strong to medium-weathered mudstone with complete rock mass and developed local cracks
Wanzhou Fuma Yangtze River Bridge (2017)	TTA is adopted on the south bank of the bridge. The length of plug body is 35 m, and the rock mass of anchorage site is interbedded with soft to relatively soft mudstone and sandstone, and broken rock mass
Jindong Bridge of Jinsha River (2017)	TTA is adopted on the east bank of the bridge. The length of the plug mass is 40 m, and the rock mass of anchorage site is composed of carbonaceous phyllite with sandstone intercalation
Luding Dadu River Bridge (2018)	TTA is adopted on the Ya'an bank of the bridge. The length of the plug body is 39.2 m, and the rock mass of anchorage site is composed of medium to strong weathered monzonitic granite
Shuibuya Qingjiang Bridge (2019)	TTA is adopted on both banks of the bridge. The length of the plug bodies is 18 m. The rock mass of anchorage site is limestone and the karst problems are prominent
Lixiang Railway Jinsha River Bridge (2019)	TTA is adopted on both banks of the bridge. The length of plug body is 45 m. The rock mass of anchorage site on the Shangri-La bank is mainly composed of thin to medium thick slate and sheet physicochemical basalt with schistatic development. The rock mass of anchorage site on the Lijiang bank is mainly composed of thick moraine
Qujiang Landscape Bridge (2019)	TTA is adopted on the north bank of the bridge. The length of plug body is 40 m, and the rock mass of anchorage site is composed of soft to relatively soft weathered sandy mudstone
Chishui River Bridge (2019)	TTA is adopted on the Sichuan bank of the bridge. The length of plug body is 78 m, and the rock mass of anchorage site is composed of mudstone and limestone
Wujiagang Yangtze River Bridge (expected to be open to traffic in 2020)	TTA is adopted on the north bank of the bridge. The length of plug body is 45 m, and the rock mass of anchorage site is composed of soft rock breeze with good integrity
Taihong Yangtze river bridge (expected to be open to traffic in 2020)	TTA is adopted on the north bank of the bridge. The length of plug body is 40 m, and the rock mass of anchorage site is soft to extreme soft mudstone (easy to soften in the presence of water)
Yaoxi Yangtze River Bridge (expected to be open to traffic in 2021)	TTA is adopted on the north bank of the bridge. The length of plug body is 40 m, and the anchorage site is composed of medium-weathered quartz sandstone, which is soft rock
Jinan Jinsha River Bridge (expected to be open to traffic in 2022)	TTA is adopted on both banks of the bridge. The length of plug body is 40 m, and the rock mass of anchorage site is mainly composed of basalt, which contains multilayer weak intercalation
Tsing Lung Bridge (expected to be open to traffic in 2022)	TTA is planned to be adopted on the north bank of the bridge
Baotaping Bridge in Fengjie County	The length of plug body is 40 m

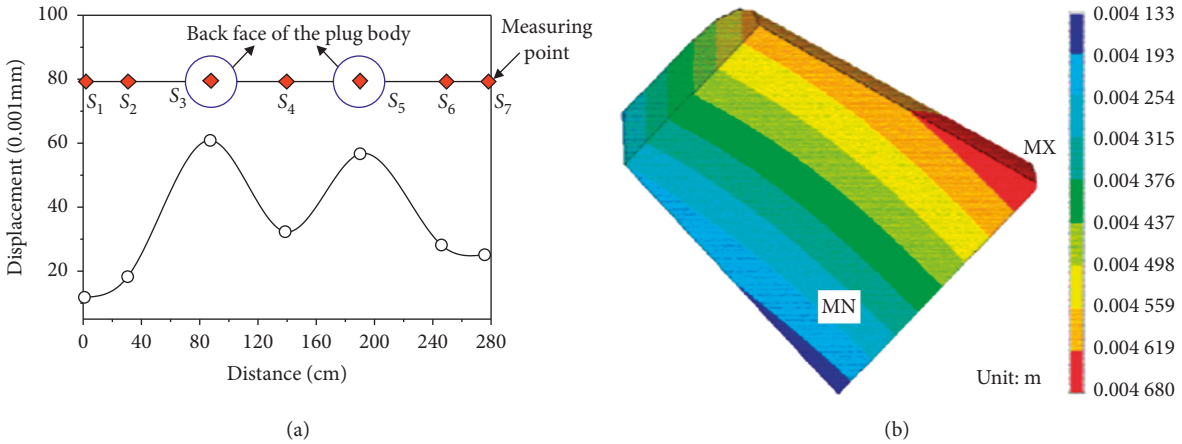

FIGURE 5: (a) Surface displacement of the rock mass on the back end of the plug body in the pull direction [33, 37]. (b) Axial displacement of plug body [41].

4.3. Effect Factors of the Mechanical Behavior of TTA. Different factors such as the size of the plug body, geometry, location as well as the stiffness ratio of rock mass to plug body will exert significant influence on the mechanical behavior of TTA.

4.3.1. Expansion Angle of Plug Body. The expansion angle βi ($i = 1$, 2, 3, and 4) is the angle between the arch of the plug body, the floor, and the side wall and the normal of the back face or front face (Figure 6). With the decrease of the β, the clamping effect of the surrounding rock to the plug body is weakened, resulting in a large displacement of the plug body in the pull direction [34, 41, 45]. With the increase of β, the peak value of the shear stress of the interface between the plug body and the surrounding rock is reduced and the local stress concentration of the plug body is improved [46].

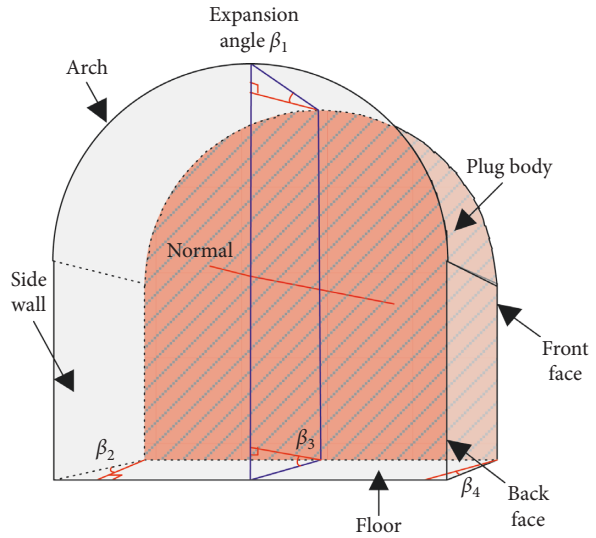

FIGURE 6: Expansion angle of plug body.

4.3.2. Length of Plug Body. When the cross-sectional area of the front face and back face of the plug body remains unchanged, the stress value of surrounding rock can be uniformly transferred and controlled, and the bearing capacity of the TTA can be appropriately improved by increasing the length of the plug body. However, as the expansion angle of plug body decreases with the increase of its length, the clamping effect of surrounding rock will be reduced indirectly by increasing the length of plug body, resulting in the increase of displacement of plug body along the pull direction [41]. Further study shows that [46] when the length of the plug body reaches a certain critical value, the increasing of the plug body length will not improve the bearing capacity of the TTA. The expansion angle is the most important factor affecting the bearing characteristics of the TTA, followed by the cross-sectional area of plug body. The length of plug body has the least effect [46].

Zhu et al. [47], based on the measured data of anchor pullout test, obtained the formula (Formula (1)) of the length of plug body through theoretical derivation. The author assumed that shear failure of TTA occurred along the interface between the plug body and the surrounding rock and did not consider the clamping effect of surrounding rock when deducing the formula of the length of anchorage plug; so it does not have an obvious advantage in terms of calculation accuracy and application range. For the interface failure mode and wedge failure mode, Liao et al. [34] established the equilibrium equation of failure surface and considered a certain safety factor. Equations (2) and (3) for calculating the length of plug body under two failure modes are obtained. The equations (2) and (3) take into account the wedge effect of the surrounding rock, which is more in line with the actual stress character of the TTA.

$$L_m \geq \frac{3\sqrt{3}Pn}{8\sqrt{C}U_p[\tau]}, \tag{1}$$

$$L_S = \frac{-R^2\gamma_1 + \sqrt{(R^2\gamma_1) + 4P_1n_1\sin\beta \cdot fk\gamma_2 R \cdot \Omega_1/\pi}}{2fk\gamma_2 R\Omega_1}, \tag{2}$$

$$L_J = \frac{-R^2\gamma_1 + \sqrt{(R^2\gamma_1) + 4P_2 n_2 \sin\beta \cdot fk\gamma_2 R \cdot \Omega_2/\pi}}{2fk\gamma_2 R\Omega_2}, \quad (3)$$

where L_m is the calculated length of the plug body when the interface failure mode occur in TTA. L_S and L_J are the calculated length of the plug body after considering safety factor when the interface failure mode and wedge failure mode occur in TTA, respectively. P, P_1, and P_2, respectively, are the ultimate pullout force when corresponding failure occurs. n, n_1, and n_2 are safety factors. C is a constant, generally taking 0.11. Up is the perimeter of the plug body. τ is the recommended value of shear strength of rock mass or plug body. γ_1 and γ_2 are the unit weight of plug bodies and surrounding rock, respectively. β is the dip angle of the main cable force. R is the radius of the cylinder that has the same height and volume with plug body. k is the coefficient of lateral earth pressure. f is the friction coefficient of interface between plug body and rock mass. Ω1 and Ω2, respectively, are the wedge effect coefficients of the interface failure mode and the wedge failure mode of TTA.

4.3.3. Section Shape and Buried Depth of Plug Body. Compared with the horse-shoe shape, the circular shape of the plug body can reduce the displacement of the TTA in the pull direction, reduce the stress concentration of the surrounding rock next to plug body, and improve the bearing capacity of the TTA [36, 46, 48]. Moreover, increasing the buried depth of plug body can effectively increase the ultimate pullout force of TTA, but there exists a critical depth, beyond which the ultimate pullout force of TTA will not increase obviously, or even decrease [37].

4.3.4. Other Factors. The dip angle of plug body has obvious effect on controlling the pull direction displacement of plug body and reducing the stress concentration of surrounding rock. The magnitude of the displacement of the plug body in the pull direction decreases as the dip angle of the plug body increases. The maximum principal stress in the surrounding rock increases first and then decreases as the dip angle of the plug body gets bigger. However, considering the interaction among the plug body, the splay saddle, and the bridge tower, bigger inclination of the plug body is not necessarily better [41, 45, 49]. On the one hand, the larger diameter of the plug body reduces the aspect ratio of the plug body, improves the tensile stiffness of the plug body, and reduces the deformation of the plug body itself. On the other hand, the contact area of the plug body with the surrounding rock is increased, which is beneficial to disperse and homogenize the stress distribution of the TTA, and thus increase the bearing capacity of the TTA [41, 46, 50].

When the elastic modulus of surrounding rock is below the critical value, increasing the elastic modulus of surrounding rock can significantly reduce the axial displacement of the plug body and the tensile stress in the rock mass. When it is above the critical value, the effect of further improving the elastic modulus of surrounding rock is not obvious. For fractured rock mass, the displacement in the pull direction of plug body can be reduced by increasing the cohesion of surrounding rock in anchorage site by grouting [46, 51]. In addition, the roughness of interface and lateral earth pressure coefficient will affect the clamping effect of surrounding rock, and thus affect the load transfer character and deformation evolution process of TTA [34].

5. Failure Modes

It is significantly important to investigate the cracking behavior of geotechnical structure during loading [52–54]. Based on the mechanical analyses and the research results of related scholars, this paper divides the failure mode of TTA into four types: slope slip failure mode, interface failure mode, wedge failure mode, and combination failure mode.

5.1. Slope Slip Failure Mode. When the structural planes of rock mass is developed and the rock mass is broken due to planes and joints cutting, the main cable force is transferred to the surrounding rock through the plug body, which will cause the slip failure of slope along the preferred structural plane, and the sliding mass to slip out together with the plug body. This kind of failure mode is known as the slip failure mode of the slope in the anchorage site, as shown in Figure 7.

Cheng et al. [55], according to the results of field model test, divided the slope slip failure into two types: one is the step sliding surface formed by two sets of structural planes (Figure 7(a)), and the other is the antidip plane sliding surface formed by cutting off the rock bridge along the gently dipping structural plane (Figure 7(b)).

5.2. Interface Failure Mode. The interface failure mode is the sliding failure of the plug body along the contact surface with the surrounding rock. The essence of this failure mode is that the interface reaches the ultimate strength of resisting shear stress, a fracture band of a certain thickness immediately next to the interface is formed due to the shear stress, and the plug body is pulled out (Figure 8(a)). When the rock mass is of better integrity, the plug body is in deep lying and the binding degree between the surrounding rock and plug body is lower. This kind of failure mode can easily occur in TTA [46].

How to improve the mechanical properties of the interface is the key to prevent this kind of failure. Jiang [46], through indoor model tests, found that adding antislip teeth to the plug body can improve the ultimate bearing capacity of TTA to a certain extent, and optimize the load transfer process between the plug body and surrounding rock. At present, there are few researches on the action mechanism of plug body with toothed pit, and it is difficult to carry out in the site construction; so, the effect of toothed pit needs to be further verified.

5.3. Wedge Failure Mode. Under the action of the main cable force, the rock mass in a certain range around the plug body tends to migrate in the direction of load, and the rock mass in this range is in the state of "tension-shear" stress. When

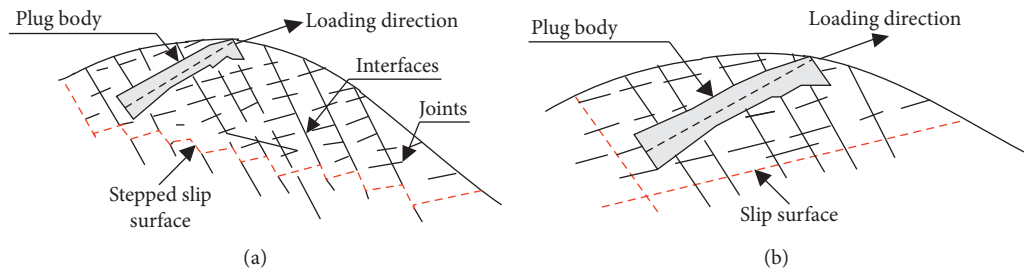

Figure 7: Slope slip failure mode. (a) Step sliding failure mode. (b) Antidip plane sliding failure mode.

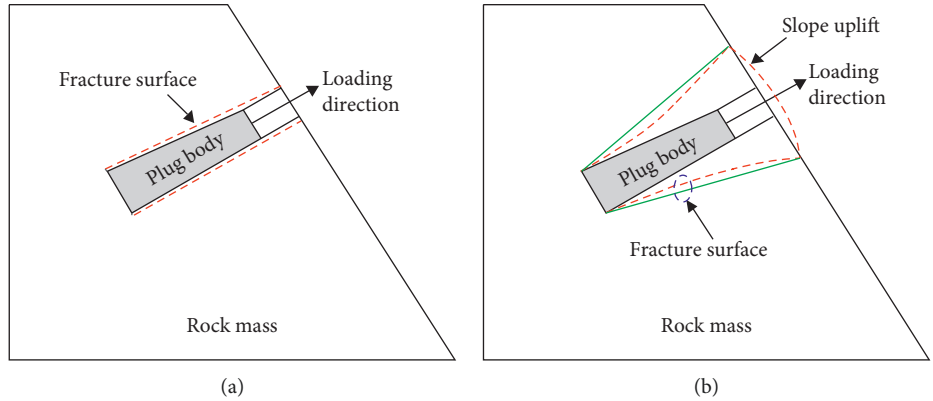

Figure 8: (a) Interface failure mode and (b) wedge failure mode.

the stress reaches its yield limit at a certain point in the rock, the initial crack occurs in the rock from that point. By increasing the load, the crack propagates continuously along the direction of tensile force and the circumferential direction of the plug body and ultimately passes through. The shape of the fracture surface can be a plane or a curved surface, which is related to the mechanical and structural characteristics of rock mass in the anchorage site. The final shape of the TTA is similar to a wedge (as shown in Figure 8(b)).

Zhang et al. [33] believes that the clamping effect of surrounding rock determines that failure will not occur on the interface. Hu et al. [40] and Tang et al. [56] studied the failure mechanism of TTAs and also obtained the wedge failure mode. However, it should be emphasized that the shape and depth of plug body, the strength and integrity of rock mass, the mechanical properties of interface, and other factors will affect the bearing deformation characteristics of TTA and then affect or even change the failure mode of the TTA. Therefore, the main control factors affecting the stability of the TTA should be determined based on the actual conditions in the field, and the possible failure modes of the TTA should be analyzed. Besides, what reinforcement measures should to be taken to prevent the occurrence of failure is a problem to be considered. For example, for the interface failure mode, technical measures that can enhance the mechanical strength of the interface should be focused on; for the wedge failure mode, the feasibility of supporting potential fracture surface by taking supporting measures such as "three-high" (i.e. high strength, high stiffness, and high prestress) anchor and small diameter prestressed anchor cable should be studied. The combination failure mode of TTAs is described in Section 6.2.

6. Calculation Method of Uplift Resistance of TTA

6.1. Normative Method. In 2002, the Code for Design of Suspension Bridges [10] was compiled by the concerning department of China, but the formula for calculating the uplift resistance of TTAs was not specified; however, an indirect formula for calculating the ultimate uplift resistance of TTAs was put forward in the Code for Design of Highway Suspension Bridges promulgated and implemented since 2015 [10]:

$$K = \frac{\left(f' W_F + C' A + W_L\right)}{P}, \tag{4}$$

where P is the design tensile force, K is the stability coefficient, f' is the friction coefficient of interface between plug body and rock mass, C' is the cohesion of the interface, A is the area of the interface, W_F is the component of the structure's own weight in the direction perpendicular to the sliding surface, and W_L is the component of the structural self-weight along the pulling direction. The molecules in the formula (4) can be equal to the ultimate pullout force of TTA, but the shear strength of the interface and structural self-weight are only considered in the formula, and the clamping effect of surrounding rock is neglected, which seriously underestimates the bearing capacity of TTAs.

6.2. Limit Equilibrium Method. On the basis of field and indoor model tests, respectively, Jiang [46] and Wang [51, 57] put forward the calculation method of ultimate pullout force of TTAs with interface failure mode by using limit equilibrium theory. The calculation model of the ultimate pullout force of TTAs with interface failure mode used by Wang Haibin and Jiang Nan are shown in Figures 9(a) and 9(b), respectively.

$$\text{Wang Haibin}: P_u K = \xi \sum_{i=1}^{3} \eta_i \left(N_i \sin \alpha_i + T_i \cos \alpha_i\right) + P_\alpha + W \sin \alpha, \quad (5)$$

$$\text{Jiang Nan}: P_u = \sum_{i=1}^{4} \left(T_i \cos \beta_i + N_i \sin \beta_i\right) + W \sin \alpha, \quad (6)$$

where P_u is the resultant force of the main cable force; P_α is the reaction force provided by the prestressed anchor cable; K is the safety factor of local shear failure of anchorage, generally taking 1.5~2.5; ηi is the lateral earth pressure coefficient; Ni and Ti ($i = 1$, 2 and 3) are equivalent normal loads and frictional resistance acting on the interface of plug body and surrounding rock on arch, floor, and side wall, respectively; β is the expansion angle of the plug body; W is the self-weight of plug body; αi is the dip angle of plug body; and ξ is the Poisson effect coefficient of plug body. In Formula (6), P_u is the ultimate pullout force of TTA; βi ($i = 1$, 2, 3, 4) is the expansion angle of the arch, left-side wall, right-side wall, and floor of plug body, respectively; W is the self-weight of plug body; α is dip angle of plug body; and Ni is the normal resultant force acting on the arch, the left-side wall, the right-side wall, and the floor of the plug body. Furthermore, Jiang [46] simplifies the curved fracture surface to straight fracture surface in order to calculate the ultimate pullout force of TTAs with a wedge failure mode (See Figure 10), by equation (7).

$$P_u = \frac{W \sin(\theta + \alpha - 90^\circ) + W|\cos(\theta + \alpha - 90^\circ)|\tan \varphi + cA'}{\sin \theta + \cos \theta \tan \varphi}, \quad (7)$$

where c is the cohesion of surrounding rock, φ is the internal friction angle of surrounding rock, and A' is the effective contact area of the bottom sliding surface. The other parameters are the same as (6).

The Poisson effect of the plug body and the effect of surrounding rock pressure on the interface are considered in formula (5). Comparing formula (5) with formula (6), the formula (5) is more reasonable. Besides, Wang [51] suggested that ηi can be calculated according to the passive earth pressure coefficient KP.

Studying the failure mode of wall rock with wedge shape (Figure 11), Zhang and Li, et al. [58, 59], by referring to the calculation method of antipulling pile and adopting force system balance method, proposed a method for calculating the ultimate pullout resistance of TTA. According to this method, the tensile force of TTA is mainly provided by shear stress, normal stress, and gravity of rock mass and plug body in the rupture area, as shown in formula (8).

$$P = (W_1 + W_2)\sin \alpha + T \cos(\gamma - \beta) + N \sin(\gamma - \beta), \quad (8)$$

where P is the ultimate pullout force, W_1 is the weight of plug body, W_2 is the weight of the surrounding rock within the failure surface, N is the resultant force of normal stress on the fracture surface, T is the resultant force of shear stress on the fracture surface, α is the dip angle of the plug body, γ is expansion angle of fracture surface, and β is the expansion angle of the plug body. The normal stress and shear stress on the fracture surface are obtained by the numerical calculation using finite element method or discrete element method, and the clamping effect of surrounding rock is considered to some extent. The formula is generally suitable for hard rock strata with no obvious geological structures.

In calculating the ultimate pullout force of TTAs, it is assumed that the normal pressure on the fracture surface is mainly caused by the self-weight of the surrounding rock and the plug body [60]. However, there is a complex interaction between the plug body and the surrounding rock under the action of the main cable force and it needs to be verified. Liao et al. [34], based on the assumption of homogeneous surrounding rock and the Mohr–Coulomb strength criterion, simplified the TTA into a plane mechanics model of variable cross-section, and obtained the formulas for calculating ultimate pullout force of TTA with the interface failure mode and wedge failure mode, respectively. The lateral earth pressure coefficient was used to calculate the normal stress and shear stress of the fracture surface in formulas that were derived by Liao et al. in reference [34]. However, the complex stress distribution on the fracture surface caused by the clamping effect formulas was ignored [58].

The ultimate pullout force of TTA can be obtained by establishing a balance equation on the fracture surface, but is based on the premise of a complete knowledge of the stress distribution on the fracture surface. At present, there are two main methods for obtaining fracture surface stress: one is numerical simulation method [58], and the other is to equate the normal stress on the fracture surface with the surrounding rock pressure and calculate the surrounding rock pressure according to the code [61]. It is not hard to see that the stress redistribution of surrounding rock caused by tunnel excavation and the influence of the interaction between plug body and surrounding rock on the stress distribution of failure surface under the action of main cable force are neglected for the second method. Therefore, the calculated results do not reflect the clamping effect of the surrounding rock, which happens to be one of the important components of the ultimate pullout force of the TTA.

6.3. Other Methods. Currently, some design institutes calculate the ultimate pullout force of TTA by using the method that is used to calculate the ultimate pullout force of GTA in China [35, 62]. This calculation method is very different from the bearing mechanism of TTA; so, it can only be used for rough estimation of the ultimate pullout force.

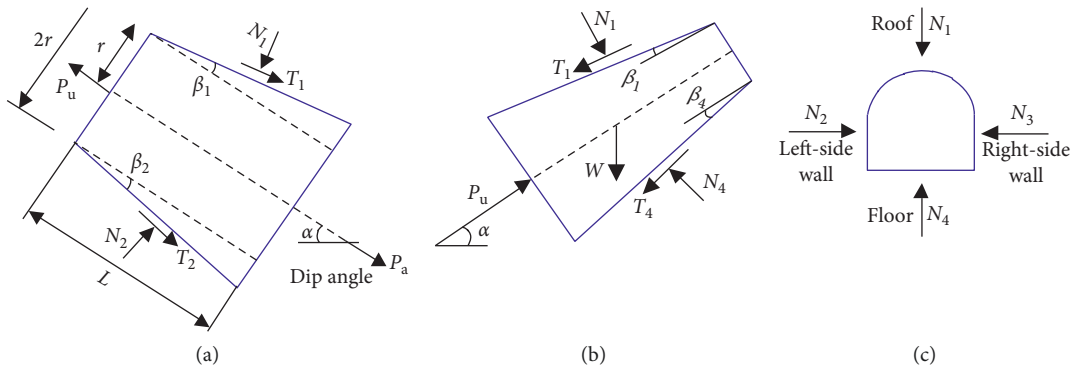

Figure 9: The calculation model of the of ultimate pullout force of TTAs with interface failure mode. (a) Wang [51, 57] and (b) Jiang [46].

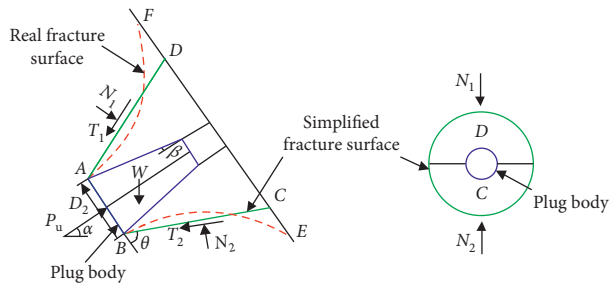

Figure 10: Schematic of the stress of TTAs with a wedge failure mode.

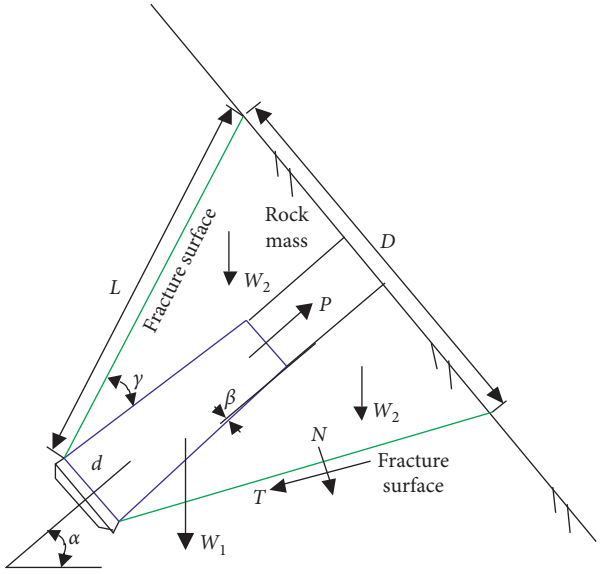

Figure 11: Computational model of ultimate pullout force of TTA with a wedge failure mode.

To sum up, obtaining the stress distribution of the fracture surface is the key to calculate the ultimate pullout force of TTA. At present, most scholars equate the normal stress on the fracture surface of the TTA with the normal pressure of surrounding rock, and calculate the surrounding rock pressure according to the code [61]. Obviously, they ignore the complexity of the stress distribution caused by the clamping effect of surrounding rock, which leads to a large error between the calculation result and the actual pullout force. Therefore, which research or test methods to adopt in order to obtain the stress distribution on the fracture surface of TTA is to be further studied.

7. Mechanical Behaviors of TTAs in Soft Rock Strata

In recent years, the author and Chongqing Branch of the Yangtze River Academy of Sciences of China worked together to carry out four field model tests to study the mechanical behaviors, such as deformation evolution law, bearing characteristics, failure modes, and long-term stability, of TTAs in soft rock strata [8, 36, 38, 39, 63–67]. This section summarizes the researches on soft rock TTA and some of the results obtained in order to provide a reference for the future studies of such TTAs.

7.1. Model Tests of TTAs in Soft Rock Strata. The research subjects are the Taihong Yangtze River Bridge (TYRB) and Jijiang Yangtze River Bridge (JYRB) in Chongqing, China. Four field model tests were performed to study the mechanical behaviors of TTAs in soft rock strata. The information of the field model test is shown in Table 2 and Figures 12(a)–12(d).

7.2. Results

7.2.1. Loading-Deformation Characteristics. The Table 3 shows the loading test results of TTAs in soft rock. As can be seen, the yield strength of surrounding rock is between 5.25P and 8.00P (P is the design load), and the peak strength is between 7.81P and 11.50P. The load-carrying capacity of TTAs in soft rock is much lower than that of TTAs in hard rock (the surrounding rock is still in the elastic stage under 50P load in Ref. [21]), but it can still bear drawing force several times as much as the design load.

Besides, water has an obvious weakening effect on the bearing capacity of TTAs in soft rock dominated by mudstone. When the water content of the surrounding rock increases from 5.36% to 7.39%, the peak strength of the anchorage decreases by 21.9%. For the TTAs built along the river, the water content of surrounding rock in the

Table 2: Field model test of the TTA built in soft rock strata.

Geological conditions	Geometric similarity ratio	Test content
The plug body is located in soft rock strata dominated by mudstone. Part of the plug body is below the average water level of the Yangtze river. Besides, the plug body is buried shallow	30	Field model test (Figure 12(a), no. M1) was performed to study the mechanical behavior of TTAs in soft rock strata with natural water content (the natural water content of rock mass is 5.36%)
	30	Field model test (Figures 12(a) and 12(b), no. M2) on soaked TTA in soft rock strata was performed (the final water content of surrounding rock is 7.39%), and the difference in mechanical behavior between M1 and M2 was compared
	10	Field model test was performed to study the mechanical behavior of TTAs at shallow depth (the maximum depth of the plug body is 6.8 m). The test diagram is shown in Figure 12(c)
The plug body is located in soft rock strata dominated by mudstone. There is a weak interlayer beneath the plug body	10	Field model test was performed to study the mechanical behavior of TTAs with underlying weak interlayers. The test diagram is shown in Figure 12(d)

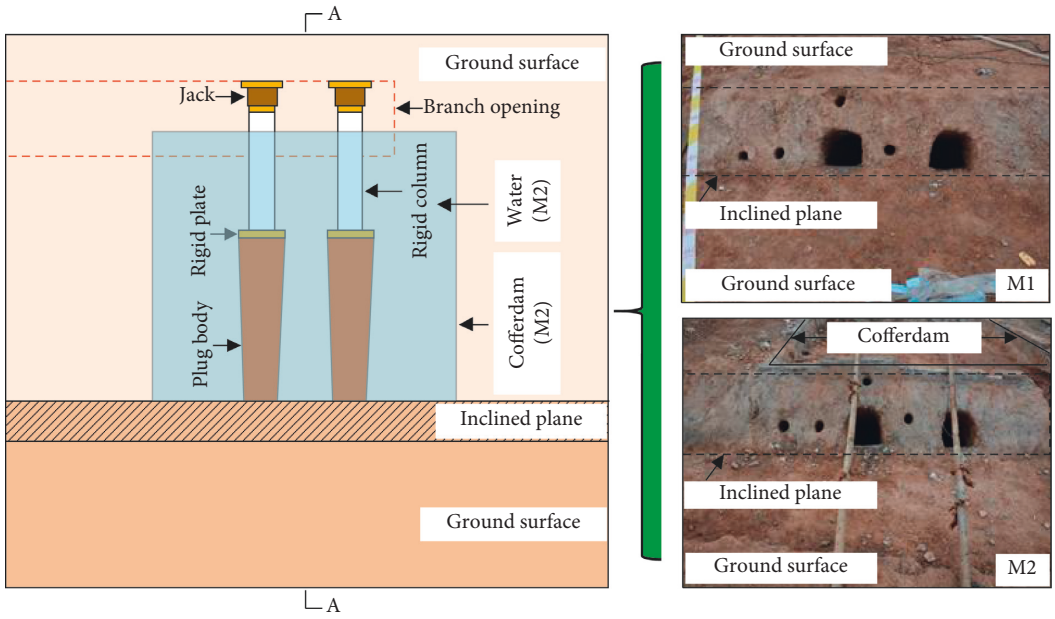

(a)

Figure 12: Continued.

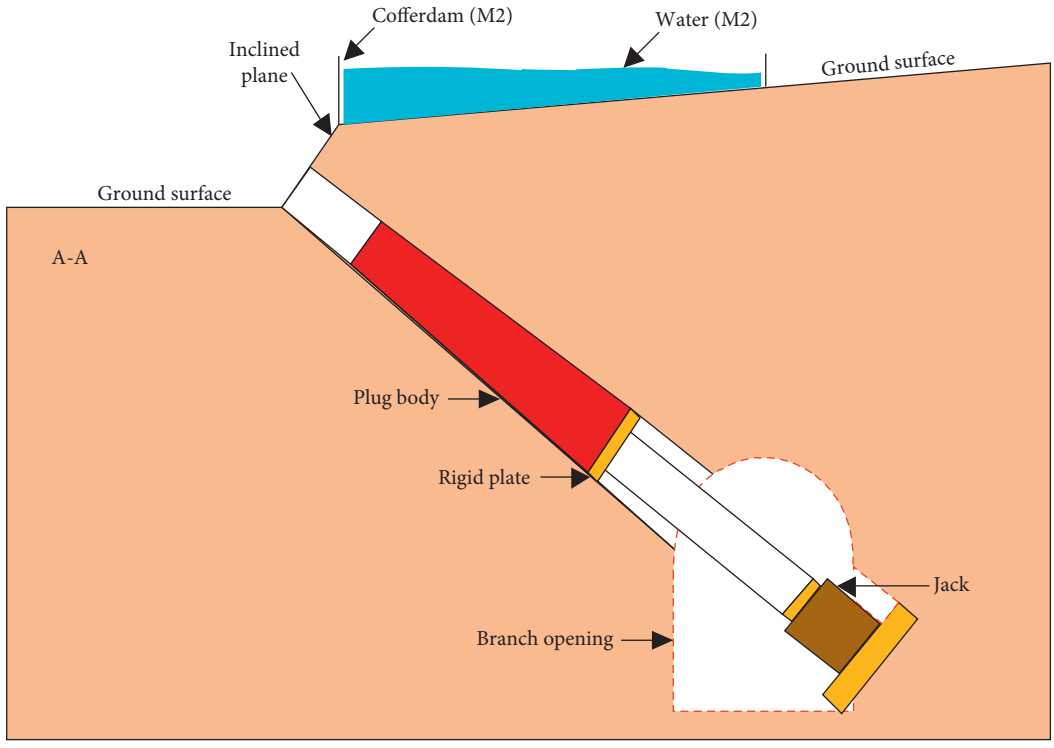

(b)

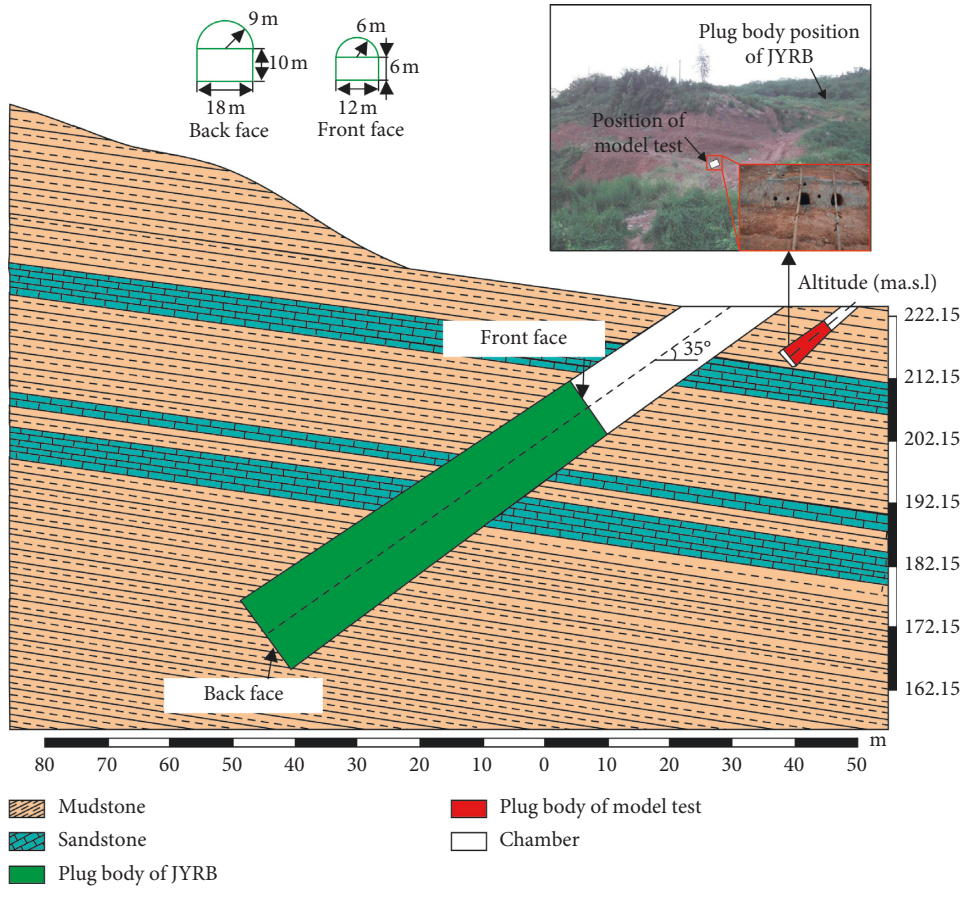

(c)

Figure 12: Continued.

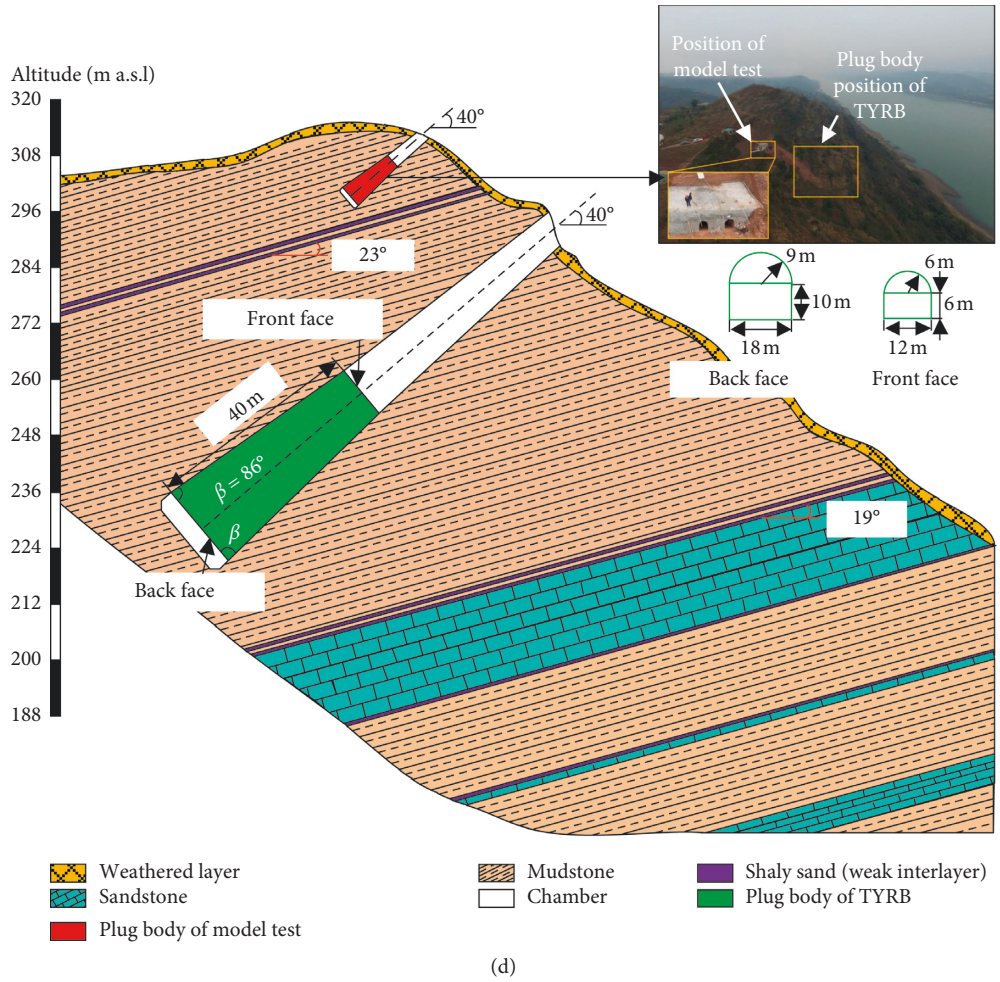

FIGURE 12: (a) Schematic of field model tests M1 and M2, (b) A-A profile, (c) stratum information and location relationship of the plug body between the model test and the JYRB, and (d) stratum information and location relationship of the plug body between the model test and the TYRB.

anchorage area fluctuates frequently, and the influence on the bearing characteristics of the TTAs should not be ignored.

In terms of surrounding rock deformation in the pull direction, different from TTAs in hard rock [30], the surface displacement distribution curve of the rock mass estimates a symmetrical bimodal at the center of the rock mass between the plug bodies [38, 39]. The surface displacement of the front face of the two plug bodies is larger compared to the rock mass between the plug bodies and on both sides of the plug bodies. Then, the control of surrounding rock deformation in the pull direction should be dominated by the surrounding rock between the left and right plug bodies. Besides, the maximum surface displacement of rock mass in the pull direction is bigger than the vertical displacement of the ground surface in the front end of the plug body. The least is the vertical displacement of the ground surface in the rear end of the plug body. The vertical deformation of the overburden at the front end of the plug body should be controlled with emphasis.

When the buried depth of the plug body is shallow, the constraint of the overburden to the plug body is reduced. Once subjected to the vertical component force transmitted by the plug body, the overburden will be easily lifted up, and then the deformation of the anchorage system in the vertical direction increases significantly. With smaller influence of rock mass on the lower part of the plug body, the deformation is smaller.

7.2.2. Long-Term Stability. The long-term performance of geotechnical structure should not be neglected [68]. One of the mains characteristics of TTAs is that it may occur creep under the long-term action of the design load (or even less than design load), while the TTA in hard rock only occur creep under the long-term action of several times the design load. Creep is one of the key factors affecting the stability of TTA in soft rock. Another important attribute is, although the long-term safety factor of TTA in soft rock is lower than that of TTA in hard rock, there is still a certain safety stock in design load, which indicates that TTA is also suitable for soft rock strata.

Table 3: The bearing test results of soft rock tunnel anchor rock [38].

Test category	Yield strength	Peak strength	Residual strength
M1 (water content 5.36%)	7.10P	10.00P	7.47P
M2 (water content 7.39%)	5.25P	7.81P	6.59P
Field model test of TTAs at shallow depth	8.00P	11.50P	—

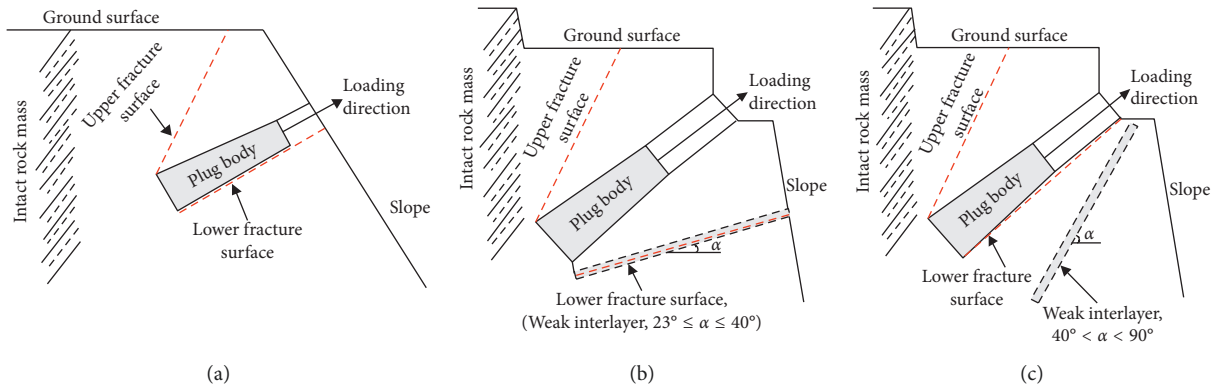

Figure 13: The failure modes of TTA under complex geological conditions [36, 38, 39, 65]: (a) shallow TTA in soft rock, (b) TTA with an underlying weak interlayer with a small dip angle, and (c) TTA with an underlying weak interlayer with a large dip angle.

7.2.3. Failure Modes. By field overload experiments and numerical simulation, the failure modes of TTAs in soft rock are obtained (Figure 13). For shallow TTAs in soft rock, because the vertical displacement of the upper rock mass of the plug body is much larger than that of the lower under the action of the main cable tension, the upper fracture surface of the plug body initiated from the rear end of the plug body to the ground surface along the direction that formed an angle with the axis of the plug body. The lower fracture surface developed along the interface between the plug body and the surrounding rock. The failure mode is generalised in Figure 13(a).

For a small dip angle ($23^\circ \le \alpha \le 40^\circ$), the study presented the same failure mode. The failure mode of the TTA in soft rock with a weak interlayer characterised with a small dip angle is unified in Figure 13(b). According to Figure 13(b), the upper fracture surface of the plug body initiated from the rear end of the plug body to the ground surface along the direction that formed an angle with the axis of the plug body. The lower fracture surface of the plug body extended along the weak interlayer.

The present study found that the TTA in soft rock with a weak interlayer characterised with a large dip angle ($40^\circ < \alpha < 90^\circ$) showed the same failure mode. The failure mode of the TTA in soft rock with a weak interlayer characterised with a small dip angle is unified in Figure 13(c). According to Figure 13(c), the upper fracture surface of the plug body initiated from the rear end of the plug body to the ground surface along the direction that formed an angle with the axis of the plug body. The fracture surface was dominated by tensile failure, and the morphology was parabolic. The lower fracture surface developed along the interface between the plug body and the surrounding rock. The final failure mode is basically consistent with that of shallow TTAs [39]. In addition, the load-bearing deformation characteristics and failure mode of shallow TTA with large dip weak interlayer in soft rock are similar to those of shallow TTA in soft rock, which indicates that the interlayer does not have much influence on TTA when the dip angle of weak interlayer is large.

8. Summary and Discussion

In this paper, the application and development trend of TTA are reviewed and the existing achievements in terms of load transfer characteristics, deformation characteristics, failure modes as well as calculation of ultimate uplift resistance are also arranged in a systematic way. Additionally, four field model tests conducted in soft rock and relevant results obtained are introduced. Some rules are drawn as follows:

(1) Based on the statistics and analysis of the anchorage forms of 113 suspension bridges in China, the trend of TTAs extending in soft rock strata and poor quality rock masses is obtained. With the help of four field model tests in soft rock (mainly composed of mudstone), the feasibility of constructing TTA in soft rock strata is verified.

(2) The failure modes of TTAs are divided into four types: slope slip failure mode, interface failure mode, wedge failure mode, and combination failure mode. The internal causes of each failure mode are analyzed.

(3) According to the surrounding rock deformation characteristics of the TTA in soft rock, the control of surrounding rock deformation in the pull direction should be dominated by the surrounding rock between the left and right plug bodies. The vertical deformation of the overburden at the front end of the plug body should be controlled with emphasis. Creep

may occur on the soft rock tunnel anchorages under the long-term action of design load (or even less than design load), and creep is one of the key factors affecting the stability of soft rock tunnel anchorage.

Although the TTA is being applied more and more in suspension bridges, the antipull mechanisms are not fully understood due to the complicated interactions between the wedge-shaped plug body and surrounding rock. A series of focused topics for future investigation that would allow to deconstruct the drivers and constraints of the development of TTA are proposed:

(1) The basic theory research lags behind the engineering application. At present, the design calculation method of TTA is not accurate enough. A key constraint on the accurate calculation of ultimate bearing capacity of TTA is the incapacity to accurately obtain the load distribution on the failure surface. Therefore, studies on the load transfer characteristics and variation law of the interface between the plug body and rock mass, analysis on the nonlinear full-history variation characteristics of the failure surface, and establishment of the numerical solution of the load distribution on the failure surface are beneficial to further improve the design and calculation method of TTA.

(2) The application condition of TTA is not clear enough, and there is a lack of design code for TTA. For this reason, it is necessary to further study the main influencing factors and rules of TTA stability under typical geological conditions, establish the general reference index with guiding significance, and explore the evaluation method and system of TTA adaptability, so as to lay a foundation for the formulation of design code for TTA.

(3) The durability of TTA needs further verification. The long-term stability of TTA under high stress and high prestress should be considered, especially for TTA in soft rock. In addition, the properties of the materials, components, and even the whole structure that constitute the TTA will degrade as time goes on under the long-term action of environment and load. Therefore, the time-varying reliability of the whole life cycle of TTA requires urgent research attention.

(4) In view of several common failure modes of TTA, the corresponding effective prereinforcement measures need to be taken.

Conflicts of Interest

The authors declare that they have no conflicts of interest.

Acknowledgments

This work was supported by the National Natural Science Foundation of China Project (41772319). The authors would also like to thank all those who contributed to the experimental part of this study.

References

[1] R. M. Liu and R. J. Zhao, "Western development: growth drive or policy trap—an analysis based on PSM-DID method," *China Industrial Economics*, vol. 6, pp. 32–43, 2015.

[2] J. Chaisse and M. Matsushita, "China's 'belt and road' initiative: mapping the world trade normative and strategic implications," *Journal of World Trade*, vol. 52, no. 1, pp. 163–185, 2018.

[3] V. Lekidis, M. Tsakiri, K. Makra, C. Karakostas, N. Klimis, and I. Sous, "Evaluation of dynamic response and local soil effects of the Evripos cable-stayed bridge using multi-sensor monitoring systems," *Engineering Geology*, vol. 79, no. 1-2, pp. 43–59, 2005.

[4] S. G. Gwon and D. H. Choi, "Static and dynamic analyses of a suspension bridge with three-dimensionally curved main cables using a continuum model," *Engineering Structures*, vol. 161, pp. 250–264, 2018.

[5] J. Q. Lei, M. Z. Zheng, and G. Y. Xu, *Suspension Bridge Design*, China Communication Press, Beijing, China, 2012.

[6] Y. Deng, A. Li, S. Chen, and D. Feng, "Serviceability assessment for long-span suspension bridge based on deflection measurements," *Structural Control and Health Monitoring*, vol. 25, no. 11, pp. 1–23, 2018.

[7] ASCE, "Long span of suspension bridge: history and performance," in *Proceedings of the ASCE National Conventions*, pp. 109–127, Boston, MA, USA, 1979.

[8] X. R. Liu, D. L. Li, X. C. Wu et al., "Filed model tests on bearing behavior of mudstone tunnel anchorage," *Chinese Journal of Geotechnical Engineering*, vol. 39, no. 1, pp. 161–169, 2017.

[9] Ö. Aydan, "Rock reinforcement and rock support," in *ISRM Book Series*, CRC Press, Taylor & Francis Group, London, UK, 2017.

[10] China Communication Press, *Industry Standard Editorial Committee of the People's Republic of China. Design Specification for Highway Suspension Bridge*, China Communication Press, Beijing, China, 2015.

[11] I. Kusano, A. Baldomir, J. Á. Jurado, and S. Hernández, "The importance of correlation among flutter derivatives for the reliability based optimum design of suspension bridges," *Engineering Structures*, vol. 173, pp. 416–428, 2018.

[12] N. K. Hong, H. M. Koh, and S. G. Hong, "Conceptual design of suspension bridges: from concept to simulation," *Journal of Computing in Civil Engineering*, vol. 30, no. 4, pp. 1–15, 2016.

[13] S. G. Gwon and D. H. Choi, "Continuum model for static and dynamic analysis of suspension bridges with a floating girder," *Journal of Bridge Engineering*, vol. 23, no. 10, pp. 1–13, 2018.

[14] A. Fenerci, O. Øiseth, and A. Rønnquist, "Long-term monitoring of wind field characteristics and dynamic response of a long-span suspension bridge in complex terrain," *Engineering Structures*, vol. 147, pp. 269–284, 2017.

[15] A. Larsen and G. L. Larose, "Dynamic wind effects on suspension and cable-stayed bridges," *Journal of Sound and Vibration*, vol. 334, pp. 2–28, 2015.

[16] S. R. Chen and J. Wu, "Modeling stochastic live load for long-span bridge based on microscopic traffic flow simulation," *Computers & Structures*, vol. 89, no. 9-10, pp. 813–824, 2011.

[17] G. S. Chen, F. Xiao, W. Zatar, and J. L. Hulsey, "Characterization of nonstationary mode interaction of bridge by considering deterioration of bearing," *Advances in Materials Science and Engineering*, vol. 2018, pp. 1–8, 2018.

[18] G. Heo, C. Kim, S. Jeon, and J. Jeon, "An experimental study of a data compression technology-based intelligent data

acquisition (IDAQ) system for structural health monitoring of a long-span bridge," *Applied Sciences*, vol. 8, no. 3, pp. 1–19, 2018.

[19] Y.-L. Xu, C. D. Zhang, S. Zhan, and B. F. Spencer, "Multi-level damage identification of a bridge structure: a combined numerical and experimental investigation," *Engineering Structures*, vol. 156, pp. 53–67, 2018.

[20] T. J. Matarazzo, P. Santi, S. N. Pakzad et al., "Crowdsensing framework for monitoring bridge vibrations using moving smartphones," *Proceedings of the IEEE*, vol. 106, no. 4, pp. 577–593, 2018.

[21] Q.-H. Zhang, Y.-J. Li, M.-W. Yu, H.-H. Hu, and J.-H. Hu, "Study of the rock foundation stability of the Aizhai suspension bridge over a deep canyon area in China," *Engineering Geology*, vol. 198, pp. 65–77, 2015.

[22] A. S. Saad, D. H. Sanders, and I. G. Buckle, "Experimental evaluation of bridge column foundation rocking behavior," *Journal of Bridge Engineering*, vol. 23, no. 11, pp. 1–13, 2018.

[23] J. W. Doig, "The best as enemy of the good: the port authority's 4th Jetport, Lindenthal's massive span over the Hudson, and the George Washington Bridge," *Journal of Urban History*, vol. 40, no. 6, pp. 1123–1137, 2014.

[24] O. H. Ammann, "George Washington Bridge: general conception and development of design," *Transactions of the American Society of Civil Engineers*, vol. 9, no. 1, pp. 56–62, 1933.

[25] J. A. Gorman, D. Gross, T. S. Hall et al., "San Francisco-Oakland Bay Bridge anchor rod cracking issues," *Materials Performance*, vol. 54, no. 6, pp. 52–57, 2015.

[26] J. Sun, R. Manzanarez, and M. Nader, "Design of looping cable anchorage system for new San Francisco-Oakland Bay Bridge main suspension span," *Journal of Bridge Engineering*, vol. 7, no. 6, pp. 315–324, 2002.

[27] K. R. Larsen, "Dehumidification slows corrosion of Forth Road bridge cables," *Materials Performance*, vol. 52, no. 4, pp. 22–24, 2013.

[28] M. Kadooka, M. Okada, Y. Hashida et al., "Cable erection of Shimotsui-Seto bridge," *KOBELCO Technology Review*, vol. 4, pp. 11–14, 1988.

[29] N. J. Gimsing and C. T. Georgakis, *Cable Supported Bridges: Concept and Design*, John Wiley and Sons, New York, NY, USA, 2011.

[30] R. D. Tovar-Valencia, A. Galvis-Castro, R. Salgado, and M. Prezzi, "Effect of surface roughness on the shaft resistance of displacement model piles in sand," *Journal of Geotechnical and Geoenvironmental Engineering*, vol. 144, no. 3, pp. 1–17, 2018.

[31] R. Nazir, H. Moayedi, A. Pratikso, and M. Mosallanezhad, "The uplift load capacity of an enlarged base pier embedded in dry sand," *Arabian Journal of Geosciences*, vol. 8, no. 9, pp. 7285–7296, 2015.

[32] S. N. M. Tafreshi, S. Javadi, and A. R. Dawson, "Influence of geocell reinforcement on uplift response of belled piles," *Acta Geotechnica*, vol. 9, no. 3, pp. 513–528, 2014.

[33] Q. H. Zhang, M. W. Yu, Z. F. Yu et al., "Field model tests on pullout capacity of tunnel-type anchorages of puli bridge," *Chinese Society for Rock Mechanics and Engineering*, vol. 34, no. 1, pp. 93–103, 2015.

[34] M. J. Liao, Q. C. Wang, C. H. Yuan et al., "Research on the pull-out capacity of the tunnel-type anchorage based on wedge-effect," *Rock and Soil Mechanics*, vol. 37, no. 1, pp. 185–193, 2016.

[35] M. W. Yu, Q. H. Zhang, Z. F. Yu et al., "Field model experiment on clamping effect of tunnel-type anchorage at puli bridge," *Chinese Society for Rock Mechanics and Engineering*, vol. 34, no. 2, pp. 261–270, 2015.

[36] D. L. Li, *The Complex Formation Shallow Buried Soft Rock Tunnel Type Anchorage is Charged*, Chongqing University, Chongqing, China, 2017.

[37] Q. Deng, H. Tang, Z. J. Wu et al., "Research on capacity characteristics of tunnel anchorage and distortion correction," *Rock and Soil Mechanics*, vol. 38, pp. 247–254, 2017.

[38] D. L. Li, X. R. Liu, X. C. Wu et al., "Research on the stability of shallow buried soft rock tunnel anchorage by in-situ model test," *Chinese Journal of Geotechnical Engineering*, vol. 39, no. 11, pp. 2078–2087, 2017.

[39] D. L. Li, X. R. Liu, H. M. Zhou et al., "Bearing behavior of tunnel anchorage in soft rock with an underlying weak interlayer," *Chinese Society for Rock Mechanics and Engineering*, vol. 36, no. 10, pp. 2457–2465, 2017.

[40] B. Hu, Q. B. Zeng, D. Rao et al., "Study on deformation law and failure mechanism of anchorage-surrounding rock system under tensile-shear complex stress-taking super-large suspension bridge on baling river for example," *Chinese Society for Rock Mechanics and Engineering*, vol. 26, no. 4, pp. 712–719, 2007.

[41] H. B. Wang, B. Gao, and Z. Sun, "Study on mechanical behaviour of tunnel anchorage system for suspension bridge," *Chinese Society for Rock Mechanics and Engineering*, vol. 24, no. 15, pp. 2728–2735, 2005.

[42] B. Z. Xiao, X. C. Wu, and C. Q. Peng, "Stability of the anchorage wall rock of tunnel for Chongqing Egongyan bridge," *Chinese Society for Rock Mechanics and Engineering*, vol. 24, no. 2, pp. 5591–5597, 2005.

[43] A. Q. Wu, Y. C. Peng, Z. J. Huang et al., "Rock mechanics comprehensive study of bearing capacity characteristics of tunnel anchorage for super-large span suspension bridge," *Chinese Society for Rock Mechanics and Engineering*, vol. 29, no. 3, pp. 433–441, 2010.

[44] B. Hu, H. B. Zhao, S. J. Wang et al., "Pull-out model test for tunnel anchorage and numerical analysis," *Rock and Soil Mechanics*, vol. 30, no. 6, pp. 1575–1582, 2009.

[45] Z. Sun, *Study on Stress Mechanism for Tunnel Anchorage*, Southwest Jiaotong University, Chengdu, China, 2005.

[46] N. Jiang, *Research on Bearing Mechanism of Tunnel Anchorage of Railway Suspension Bridge and its Calculation Method*, Southwest Jiaotong University, Chengdu, China, 2014.

[47] Y. Zhu, C. H. Liao, and J. Wei, "The length estimation formula of tunnel anchor body," in *Proceedings of the China Highway Society Bridge and Structural Engineering Branch 2005 National Bridge Academic Conference*, pp. 310–315, Hangzhou, China, 2005.

[48] N. Jiang and J. Feng, "Effect of cross section type of tunnel anchorage on its mechanical behavior for suspension bridge," *Journal of Chongqing Jiaotong University (Natural Science)*, vol. 31, no. 4, pp. 755–759, 2012.

[49] F. Q. Cheng, *Study on Bearing Capacity of Tunnel Anchorage in Large Suspension Bridge*, Southwest Jiaotong University, Chengdu, China, 2015.

[50] F. Huang, *Research on the Development Mechanism of Pile Lateral Friction Resistance under Pressure and Pull Load*, Tsinghua University, Beijing, China, 1998.

[51] H. B. Wang, *Mechanism Research of Compound Tunnel Anchorage of Suspension Bridge*, Southwest Jiaotong University, Chengdu, China, 2005.

[52] Y. Wang, X. Zhou, and M. Kou, "An improved coupled thermo-mechanic bond-based peridynamic model for cracking behaviors in brittle solids subjected to thermal

shocks," *European Journal of Mechanics-A/Solids*, vol. 73, pp. 282–305, 2019.
[53] J. Wang, W. Li, and Z. Song, "Development and implementation of new triangular finite element based on MGE theory for bi-material analysis," *Results in Physics*, vol. 13, pp. 1–9, 2019.
[54] X. Tian, Z. Song, and J. Wang, "Study on the propagation law of tunnel blasting vibration in stratum and blasting vibration reduction technology," *Soil Dynamics and Earthquake Engineering*, vol. 126, pp. 1–12, 2019.
[55] H. X. Cheng, C. C. Xia, and R. Q. Li, "Guangdong humen bridge east anchorage of rock mass stability," *Journal of Tongji University*, vol. 23, no. 3, pp. 338–342, 1995.
[56] H. Tang, X. R. Xiong, Q. Deng et al., "Deformation law and failure mechanism of anchorage-surrounding rock system of Puli extra-large bridge," *Journal of Shanghai Jiaotong University*, vol. 49, no. 7, pp. 961–967, 2015.
[57] H. B. Wang and B. Gao, "Calculation method of bearing capacity of compound tunnel anchorage system of suspension bridge," *Journal of Southeast University (Natural Science Edition)*, vol. 35, no. 1, pp. 89–94, 2005.
[58] Q. H. Zhang, Y. J. Li, M. W. Yu et al., "Preliminary study of pullout mechanisms and computational mode of pullout force for rocks surrounding tunnel-type anchorage," *Rock and Soil Mechanics*, vol. 38, no. 3, pp. 810–820, 2017.
[59] Y. Li, R. Luo, Q. Zhang, G. Xiao, L. Zhou, and Y. Zhang, "Model test and numerical simulation on the bearing mechanism of tunnel-type anchorage," *Geomechanics and Engineering*, vol. 12, no. 1, pp. 139–160, 2017.
[60] R. Zhang, *The Bearing Capacity Test of the Tunnel-type Anchorage in Soft Rock under Water Effect*, Chongqing University, Chongqing, China, 2016.
[61] China Railway Publishing House, *The Second Survey and Design Institute of Railway. Code for Design of Railway Tunnel*, China Railway Publishing House, Beijing, China, 2005.
[62] Q. H. Zhang, J. H. Hu, G. P. Chen et al., "Study of rock foundation stability of Aizhai bridge," *Chinese Society for Rock Mechanics and Engineering*, vol. 31, no. 12, pp. 2420–2430, 2012.
[63] X. C. Wu, X. R. Liu, D. L. Li et al., "Failure model test on soaked tunnel anchor in soft surrounding rock," *Rock and Soil Mechanics*, vol. 37, no. 4, pp. 1023–1030, 2016.
[64] D. L. Li, X. R. Liu, X. C. Wu et al., "Three-dimensional elastoplastic analysis on the stability of tunnel anchorage in soft rock," in *ASCE-Geotechnical Special Publication*, no. 264, pp. 166–175, Newyork, NY, USA, 2016.
[65] X. Liu, Y. Han, D. Li et al., "Anti-pull mechanisms and weak interlayer parameter sensitivity analysis of tunnel-type anchorages in soft rock with underlying weak interlayers," *Engineering Geology*, vol. 253, pp. 123–136, 2019.
[66] X. C. Wu, X. R. Liu, and D. L. Li, "The field reduced scale test on tunnel anchorage with soft surrounding rock," *Electronic Journal of Geotechnical Engineering*, vol. 20, pp. 12811–12833, 2015.
[67] Y. F. Han, X. R. Liu, D. L. Li et al., "Model test on the bearing behaviors of the tunnel-type anchorage in soft rock with underlying weak interlayers," *Bulletin of Engineering Geology and the Environment*, pp. 1–18, 2019.
[68] Z. Zhang, X. Jin, and W. Luo, "Long-term behaviors of concrete under low-concentration sulfate attack subjected to natural variation of environmental climate conditions," *Cement and Concrete Research*, vol. 116, pp. 217–230, 2019.